Document downloaded from:

http://hdl.handle.net/10251/100410

This paper must be cited as:

The final publication is available at

http://doi.org/10.1016/j.measurement.2016.05.051

Copyright Elsevier

Additional Information

DETERMINING IMAGE DISTORTION AND PBS (POINT OF BEST SYMMETRY) IN DIGITAL IMAGES USING STRAIGHT LINE MATRICES

Herráez, J.[a*], Denia, J.L.[a], Navarro, P.[b], Rodríguez, J.[c] and Martín M.T.[c]

[a] Department of Cartographic Engineering, Geodesy and Photogrammetry. School of Civil Engineering (UPV). 46022, Valencia (Spain).

[b] Department of Graphic Expression in Architecture. School of Architecture (UPV) 46022, Valencia (Spain).

[c] Polytechnic High School of Lugo. University of Santiago de Compostela. 27002, Lugo (Spain).

**Corresponding author: Address: Polytechnic University of Valencia, 46022 Valencia (Spain). Tel.: +34 963877000 Ext: 75522. Fax: +34 963877159. E-mail:jherraez@cgf.upv.es*

Abstract

It is impossible to take accurate measurements in photogrammetry without first removing the distortion in images. This paper presents a methodology for correcting radial and tangential distortion and for determining the PBS (Point of Best Symmetry) without knowledge of the interior orientation parameters (IOPs). An analytical plumb-line calibration method is used, measuring only the coordinates of points on straight lines, regardless of the position and direction of these lines within the image. Points belonging to multiple lines can also be used since the effects on their X and Y coordinates are calculated independently. The results obtained on an image of a common scene, taken with a handheld non-metric camera, show a high degree of accuracy even with a minimum number of observables. And its application on a calibrated grid for engineering purposes with a semi-metric camera, results optimal even using a single image.

Keywords: image processing, image analysis, camera calibration, plumb-lines, distortion.

1. Introduction

Camera calibration is a basic operation in many photogrammetric processes, since without knowledge of the calibration parameters it is impossible to take accurate measurements. Because of the importance of this issue, many textbooks on photogrammetry and computer vision have dealt with it extensively [1-5] as well as numerous publications in international journals [6-7].

The two basic models of camera calibration work include, firstly, those based on perspective projection by collinearity, where the IOPs are assumed to be stable and collinearity can be applied by using collections of images. These non-linear techniques provide highly accurate results using least-squares processes and allow the IOPs to be obtained [8], while linear techniques are very fast but can offer only imprecise radial distortion calculations [9]. Secondly, there are models based on the fundamental matrix, which allow changes in the IOPs but which also give unstable results. It is common for 3D objects to be used for these models because planar point arrays cannot be accommodated [10]. Although a third working model based on a combination of the previous two also exists [11-12], it is not commonly used and has been absorbed by other models based on iterative calculation [7].

Undoubtedly the most widely used mathematical model is collinearity [13-14], where the minimum quadratic fit can provide very accurate results in a single process while also providing the IOPs. However, certain conditions must exist in order to achieve such results: multiple converging photos of a 3D object with either a good geometrical point distribution or a calibration pattern with known coordinate points (in which case the photos must be orthogonal, very convergent, and taken from different distances). This method actually works well but has the disadvantage of requiring multiple images and initial values in order to solve the iterative process. The same issues occur with DLT-based work [9]. This means that the use of point-based models is much more widespread in photogrammetry while line-based models, referred to as plumb-line calibration, have not been applied as frequently or as recently [8,15-18].

However, several studies have now shown that not all of the IOPs are required in the relative orientation process for generating models, in which case it is only necessary to correct for image distortion in order for the approach to work [19]. The fact that it is possible to create 3D using algorithms independent of the IOPs means that calibration work can be reduced to the mere determination of distortion parameters. From this point of view, the use of the plumb-line method becomes optimal, since it is based on geometrical constraints on the image. A clear example of this methodology is seen in [16], where an algorithm based on the equation of a line of the type $x \cdot \cos\theta + y \cdot \sin\theta = \rho$ is proposed. This approach calls for application of prior knowledge of the θ direction of the line after the coordinates have been corrected for distortion. This entails making a rough initial calculation with a first initial value for the direction of the line, then initiating an iterative calculation process by changing the θ value in the equation in accordance with the results obtained in the previous iteration. Thus each point in the image presents an equation. It therefore follows that this method cannot be used for points belonging to two or more lines, since the same point would have different residuals depending upon the line considered. This approach is also used by [18], who use the Hough transform and calculate the points found along a straight line through θ and ρ, to later make the correction.

The present paper presents an algorithm based on the plumb-line method but developed from the equation of a straight line passing through three points. This approach involves substantial differences compared to previous ones and can treat each point independently for each coordinate (x and y), which allows a reliability test to be performed as well as independent weighting within the system. For every three points an equation is generated, which represents a reduction of two equations and two unknowns for each line (it is not necessary to know the direction of the line or its position within the image). Additionally, use of a point of intersection of two lines (a circumstance that will occur when using a calibration grid) is optimal under our methodology, although such points have been unusable in previous approaches. Furthermore, the algorithm developed allows distortion and PBS decentering to be determined even when using a single image, and it also allows different solutions to be established depending upon the accuracy to be achieved.

2. Development of the image distortion correction algorithm

The distortion algorithm will be the one that manages to rectify the curves, transforming them into straight lines. To that end, we define each line in the image by measuring at least 3 points along its route, (2 points always determine a line but they cannot determine its curvature), with these points being as far apart as possible to ensure that they are not in a straight line. Any chosen point in the image $\left(x_i', y_i'\right)$ has measured coordinates (x_{im}, y_{im}). The difference between the coordinates of the selected points and the measurement result (which will have to be corrected of radial and tangential distortion) will be given by (1):

$$\left(x_i', y_i'\right) = \left(x_{im}, y_{im}\right) + \left(dx_i + dy_i\right) + \left(dx_{PBS}, dy_{PBS}\right) \tag{1}$$

where

(dx_i, dy_i) : measurement error vector (or residual)

$(\mathrm{dx}_{\mathrm{PBS}}, \mathrm{dy}_{\mathrm{PBS}})$: coordinates of the PBS (point of best symmetry).

2.1. Obtaining the distortion equation

Definition of the radial distortion at any point *i* of an image using odd degree polynomials ($\Delta_r r_i$) is commonly given by (2):

$$\Delta_r r_i = a \cdot r_i + b \cdot r_i^3 + c \cdot r_i^5 + \ldots \tag{2}$$

where

$r_i = \sqrt{x_i'^2 + y_i'^2}$: radius vector of any point (x_i', y_i') with distortion with respect to the PBS

$a, b, c, \ldots$: radial distortion polynomial coefficients

Breaking down the value of (2) based upon the components of the radius vector, a polynomial radial distortion is obtained for each coordinate using (3):

$$\begin{aligned} \Delta_r x_i &= x_i' \cdot (a + b \cdot r_i^2 + c \cdot r_i^4 + \ldots) \\ \Delta_r y_i &= y_i' \cdot (a + b \cdot r_i^2 + c \cdot r_i^4 + \ldots) \end{aligned} \tag{3}$$

Tangential distortion would be given by (4):

$$\begin{aligned} \Delta_t x_i &= P_1 \cdot (r_i^2 + 2 \cdot x_i'^2) + 2 \cdot P_2 \cdot x_i' \cdot y_i' \\ \Delta_t y_i &= P_1 \cdot (r_i^2 + 2 \cdot y_i'^2) + 2 \cdot P_2 \cdot x_i' \cdot y_i' \end{aligned} \tag{4}$$

where

$\mathrm{P}_1, \mathrm{P}_2$: tangential distortion polynomial coefficients

Whereby, the calculation of the distortion-corrected coordinates (x_i, y_i) for any point of the image *i* results from (5):

$$\begin{aligned} x_i &= x_i' + \Delta_r x_i + \Delta_t x_i = x_i' \cdot (1 + a + b \cdot r_i^2 + c \cdot r_i^4 + \ldots) + P_1 \cdot (r_i^2 + 2 \cdot x_i'^2) + 2 \cdot P_2 \cdot x_i' \cdot y_i' \\ y_i &= y_i' + \Delta_r y_i + \Delta_t y_i = y_i' \cdot (1 + a + b \cdot r_i^2 + c \cdot r_i^4 + \ldots) + P_2 \cdot (r_i^2 + 2 \cdot y_i'^2) + 2 \cdot P_2 \cdot x_i' \cdot y_i' \end{aligned} \tag{5}$$

According to (5), the higher the value of *r,* the higher the value of the additional term will be according to the degree of the polynomial. Consequently, the number of terms used will be significant, while for smaller *r* values only the first terms will be of interest. The first term in the expression describes the start of the distortion function and the successive terms describe its variation trend.

In order to determine the distortion coefficients we will measure points on straight lines that appear in the image as curved lines. By measuring three points on a straight line $P_1(x_1, y_1)$, $P_2(x_2, y_2)$, and $P_3(x_3, y_3)$, the image coordinates must satisfy (6):

$$k = \frac{(x_2 - x_1)}{(y_2 - y_1)} - \frac{(x_3 - x_1)}{(y_3 - y_1)} = 0 \tag{6}$$

Equation 6 is linearized by Taylor polynomials (only first order) obtaining (7):

$$k_0 + \sum \frac{dk}{d\alpha} d\alpha + \sum \frac{dk}{d\beta} d\beta + \sum \frac{dk}{d\gamma} d\gamma + \sum \frac{dk}{d\xi} d\xi = 0 \tag{7}$$

where

α: decentering coordinates $(\mathrm{dx}_{\mathrm{PBS}}, \mathrm{dy}_{\mathrm{PBS}})$

β: radial distortion coefficients (a,b,c…)

γ: tangential distortion coefficients (P_1 and P_2)

ξ: resiaduals for each point (dx_i , dy_i)

being k_0 the equation value using image coordinates and initial values for α,β,γ and ξ.

Substituting (5) into the linearized (7) we obtain (8):

$$\begin{aligned} &k_0 + \left(k_1^0 \cdot dx_{PBS} + k_2^0 \cdot dy_{PBS}\right) + \left(k_1^1 \cdot a + k_2^1 \cdot b + k_3^1 \cdot c + \ldots\right) + \left(k_1^2 \cdot P_1 + k_2^2 \cdot P_2\right) + \\ &+ \left(k_1 \cdot dx_0 + k_2 \cdot dy_0 + k_3 \cdot dx_1 + k_4 \cdot dy_1 + k_5 \cdot dx_2 + k_6 \cdot dy_2\right) = 0 \end{aligned} \tag{8}$$

where

$$k_0 = \left[\left(x_{2m} - x_{1m}\right)\cdot\left(y_{3m} - y_{1m}\right) - \left(x_{3m} - x_{1m}\right)\cdot\left(y_{2m} - y_{1m}\right)\right]$$

PBS decentering coefficients:

$$k_1^0 = \left(b\cdot r_2^2 + c\cdot r_2^4 + \ldots. - b\cdot r_1^2 - c\cdot r_1^4 - \ldots\right)\cdot\left(y_{3m} - y_{1m}\right) - \left(b\cdot r_3^2 + c\cdot r_3^4 + \ldots. - b\cdot r_1^2 - c\cdot r_1^4 - \ldots\right)\cdot\left(y_{3m} - y_{1m}\right)$$

$$k_2^0 = \left(x_{2m} - x_{1m}\right)\cdot\left(b\cdot r_3^2 + c\cdot r_3^4 + \ldots. - b\cdot r_1^2 - c\cdot r_1^4 - \ldots\right) - \left(x_{3m} - x_{1m}\right)\cdot\left(b\cdot r_2^2 + c\cdot r_2^4 + \ldots. - b\cdot r_1^2 - c\cdot r_1^4 - \ldots\right)$$

Radial distortion coefficients:

$$k_1^1 = \left[\left(x_{2m} - x_{1m}\right)\cdot\left(y_{3m} - y_{1m}\right) - \left(x_{3m} - x_{1m}\right)\cdot\left(y_{2m} - y_{1m}\right)\right]$$

$$\begin{aligned} k_2^1 = [&\left(x_{2m}\cdot r_2^2 - x_{1m}\cdot r_1^2\right)\cdot\left(y_{3m} - y_{1m}\right) + \left(x_{2m} - x_{1m}\right)\cdot\left(y_{3m}\cdot r_3^2 - y_{1m}\cdot r_1^2\right) - \\ &- \left(x_{3m}\cdot r_3^2 - x_{1m}\cdot r_1^2\right)\cdot\left(y_{2m} - y_{1m}\right) + \left(x_{3m} - x_{1m}\right)\cdot\left(y_{2m}\cdot r_2^2 - y_{1m}\cdot r_1^2\right)] \end{aligned}$$

$$\begin{aligned} k_3^1 = [&\left(x_{2m}\cdot r_2^4 - x_{1m}\cdot r_1^4\right)\cdot\left(y_{3m} - y_{1m}\right) + \left(x_{2m} - x_{1m}\right)\cdot\left(y_{3m}\cdot r_3^4 - y_{1m}\cdot r_1^4\right) - \\ &- \left(x_{3m}\cdot r_3^4 - x_{1m}\cdot r_1^4\right)\cdot\left(y_{2m} - y_{1m}\right) + \left(x_{3m} - x_{1m}\right)\cdot\left(y_{2m}\cdot r_2^4 - y_{1m}\cdot r_1^4\right)] \end{aligned}$$

Tangential distortion coefficients:

$$\begin{aligned} k_1^2 = &\left(r_2^2 + 2\cdot x_2^2 - r_1^2 - 2\cdot x_1^2\right)\cdot\left(y_{3m} - y_{1m}\right) + \left(x_{2m} - x_{1m}\right)\cdot\left(2\cdot x_3\cdot y_3 - 2\cdot x_1\cdot y_1\right) - \\ &- \left(r_3^2 + 2\cdot x_3^2 - r_1^2 - 2\cdot x_1^2\right)\cdot\left(y_{2m} - y_{1m}\right) + \left(x_{3m} - x_{1m}\right)\cdot\left(2\cdot x_2\cdot y_2 - 2\cdot x_1\cdot y_1\right) \end{aligned}$$

$$k_2^2 = \left(r_3^2 + 2\cdot y_3^2 - r_1^2 - 2\cdot y_1^2\right)\cdot\left(x_{2m} - x_{1m}\right) + \left(y_{3m} - y_{1m}\right)\cdot\left(2\cdot x_2\cdot y_2 - 2\cdot x_1\cdot y_1\right) -$$
$$- \left(r_2^2 + 2\cdot y_2^2 - r_1^2 - 2\cdot y_1^2\right)\cdot\left(x_{3m} - x_{1m}\right) - \left(y_{2m} - y_{1m}\right)\cdot\left(2\cdot x_3\cdot y_3 - 2\cdot x_1\cdot y_1\right)$$

Coefficients of measurement error (residuals):

$$k_1 = -\left[(y_{2m} - y_{1m}) + (y_{3m} - y_{1m})\right]$$

$$k_2 = -\left[(x_{2m} - x_{1m}) + (x_{3m} - x_{1m})\right]$$

$$k_3 = (y_{3m} - y_{1m})$$

$$k_4 = (x_{3m} - x_{1m})$$

$$k_5 = (y_{2m} - y_{1m})$$

$$k_6 = (x_{2m} - x_{1m})$$

2.2. Analysis of the coefficients and particularization of the equation

The independent term k_0 shows the numerical misalignment of the three points studied. Since the distortion causes small displacements in the image, the coefficient k_1^1 will yield a value that is practically zero, which means that it cannot provide a reliable value according to our equation. This result is logical since the coefficient multiplies the coordinates in a linear manner (x_{im}, y_{im}), so that just by taking its value into account, a valuable scale factor is obtained for the image $(1+a)$. In order for the 3 points studied to be in a straight line, the only possible scale factor corresponds to a value $a = -1$, an absurdly trivial solution. Accordingly, we dispense with the value *a*, assigning it a null value because it does not affect the calculation. The application of the formulation developed for determining the distortion can be split into four specific cases as presented below.

2.2.1. Definition of a straight line with 3 points

With three points, only a single equation with a single coefficient is possible (a determinate system with a single solution). The particularized (8) results as $k_0 + k_1^1\cdot a + k_2^1\cdot b + k_3^1\cdot c = 0$ where $k_1^1 = 0$ according to the established hypothesis. The distortion equation is reduced according to (9):

$$k_0 + k_2^1\cdot b = 0 \tag{9}$$

where $b = -k_2^1 / k_0$ since the expression allows the calculation of a single coefficient and requires *c*, as well as the differential coefficients, to take on a null value because the system becomes determinate.

2.2.2. Definition of a straight line with 4 points.

With four points we can propose two equations with two coefficients, *b* and *c* (a determinate system with a single solution). The calculation consists of generating a simple system of two equations with two unknowns, which results from applying (8) to the first 3 and last 3 points. The resulting values would be derived according to (10):

$$b = \frac{-\left(k_0 + k_3^1 \cdot c\right)}{k_2^1} \qquad c = \frac{-\left(k_0 + k_2^1 \cdot b\right)}{k_3^1} \tag{10}$$

2.2.3. Definition of a straight line with more than 4 points.

Calculating more than two coefficients is not reliable in the case of digital images, since the value of all coefficients after the third (*d* and subsequent) influence the distortion correction only within a pixel (geometric information obtained with the accuracy of a single pixel cannot have a determining effect). However, an approach where more than two coefficients are obtained allows us to determine the consistency of the values obtained using reliability tests, while study of the covariance matrix enables us to determine the accuracy and consistency obtained for the coefficients.

The number proposed for (8) for the distortion calculation will be *n-2,* with *n* being the number of measured points. This produces a redundant iterative system of *n-2* equations and as many unknowns as the number of coefficients we wish to determine. The system of equations obtained is the one shown below as (11). Its resolution by least squares will obtain the coefficients as well as the residuals for each of the measured coordinates. Finally, covariance and cofactor matrices will be obtained and internal and external reliability tests can then be applied to the resulting solution:

$$[A]\cdot[X]+[B]\cdot[R]=[L] \tag{11}$$

where

$[A]=\begin{bmatrix} A_{1,1} & \dots & A_{n,1} \\ \dots & \dots & \dots \\ A_{1,n-2} & \dots & A_{n,n-2} \end{bmatrix}$: matrix of coefficients of the unknowns

$[X]=\begin{bmatrix} b \\ c \end{bmatrix}$: vector of unknowns

[B]: matrix of coefficients of the residuals, a dispersed matrix that only has 6 non-zero coefficients per row (corresponding to the columns belonging to the three points used in the equation that builds the row).

$$\left[R\right]=\begin{bmatrix} dx_1 \\ ... \\ dy_n \end{bmatrix}$$: residual vector with *2n* rows.

$$\left[L\right]=\begin{bmatrix} L_{0,1} \\ ... \\ L_{0,n-2} \end{bmatrix}$$: vector of independent terms with *n-2* rows.

To solve the system we need to establish the weight matrix of the residuals [*P*]. If all points have been measured with the same accuracy, [*P*] results a square matrix with the dimensions *(2·n,2·n)*. This matrix is arranged so that each coordinate has an integer weight, being P(i,i)=1 if each coordinate has the same weight and P(i,j)=0 for the rest (being i and j the files and columns of the matrix respectively). However, it is possible to reduce the accuracy of any point by lowering the unit value corresponding to its row. Although the resolution of the system is independent of the order in which the points are raised and ordered, the two most extreme points on the straight line should be used in all equations, taking one of the others as the third point.

The solution for [X] will be given by minimizing [R] in equation (11) through Lagrange coefficients [λ] (12):

$$\begin{aligned}\left[X\right]&=\left[S\right]^{-1}\cdot\left[A\right]^{t}\cdot\left[M\right]^{-1}\cdot\left[L\right]\\ \left[R\right]&=\left[P\right]^{-1}\cdot\left[B\right]^{t}\cdot\left[\lambda\right]\end{aligned} \tag{12}$$

where

$$\begin{aligned}\left[S\right]&=\left[A\right]^{t}\cdot\left[M\right]^{-1}\cdot\left[A\right]\\ \left[M\right]&=\left[B\right]\cdot\left[P\right]\cdot\left[B\right]^{t}\\ \left[\lambda\right]&=-\left[M\right]^{-1}\cdot\left(\left[A\right]\cdot\left[X\right]-\left[L\right]\right)\end{aligned}$$

The cofactor matrices $[Q_{xx}],[Q_{rr}]$ and covariance matrices $[\sigma_{xx}],[\sigma_{rr}]$ of [X] and [R] that allow us to analyze the solution are given by (13):

$$\begin{aligned}\left[Q_{xx}\right]&=\left[S\right]^{-1}\\ \left[Q_{rr}\right]&=\left[P\right]^{-1}\cdot\left[B\right]^{t}\cdot\left[M\right]^{-1}\cdot\left[H\right]\cdot\left[M\right]^{-1}\cdot\left[B\right]\cdot\left[P\right]\\ \left[\sigma_{xx}\right]&=\sigma_0^2\cdot\left[Q_{xx}\right]\\ \left[\sigma_{rr}\right]&=\sigma_0^2\cdot\left[Q_{rr}\right]\end{aligned} \tag{13}$$

where,

$$[H]=[I]-\left([A]\cdot[S]^{-1}\cdot[A]^{t}\cdot[M]^{-1}\right)$$

$$\sigma_0^2=\frac{[R]^t\cdot[P]\cdot[R]}{N_E-N_C}$$

and where N_E is the number of equations and N_C is the number of coefficients to be determined (usually two: *b* and *c*).

2.2.4. Definition of multiple straight lines with more than 4 points in each

If each line *i* is defined by n_i points then we can define n_i-*2* equations for each line, forming a system of equations with as many unknowns as the number of coefficients we wish to determine. The system calculation is carried out through (11), taking into account that the vector of unknowns now yields (14):

$$[X]=\begin{bmatrix} b \\ c \\ P_1 \\ P_2 \\ dx_{PBS} \\ dy_{PBS} \end{bmatrix} \tag{14}$$

Everything expressed above with respect to (12) and (13) remains valid in relation to reliability, accuracy of the results, and number of coefficients that we are able to determine.

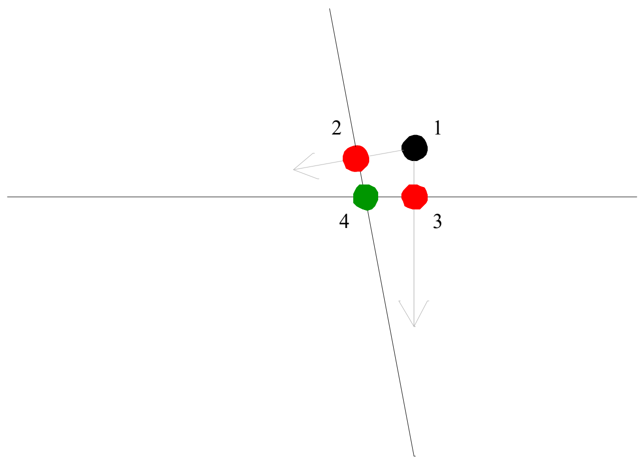

Figure 1. Point 1: point corrected for distortion using a residual for measurement error. Points 2 and 3: corrected positions for point 1 by the conventional method based upon the straight line studied. Point 4: position of point 1 corrected using the new algorithm, Eq. (8).

The proposed calculation allows the use of points belonging to multiple lines simultaneously, taking into account the fact that each point must have a unique residual for each coordinate (dx_i or dy_i), the unknowns of which must be in vector [R]. In contrast, in the traditional methods an algorithm is proposed based upon the equation of a line of the type $x \cdot \cos\theta + y \cdot \sin\theta = \rho$ [16]. For its resolution a residual is added to the equation in the direction perpendicular to the straight line. The solutions for the system allow the minimum value of the corrections for the measured points to be obtained so that they are aligned after the correction is applied.

However, the correction for x and y must be analyzed independently in order to obtain the minimum displacement that will align the points, using (8). The traditional methods present a problem when a point belongs to multiple straight lines. In such cases, resolution of the system provides a different residual value for the same point on the different lines (Fig. 1). Since it is not possible to use a single residual value to correct the position of the point for all of the lines at once, these points will end up being inconsistent and will become unusable. In the case where grids are used (the usual case in calibration), all of the points belong to multiple straight lines. This means that the traditional method will generate multiple equations under erroneous conditions compared to the algorithm developed in the present work. When applying (8), the unknowns are unique for each point, regardless of whether the point belongs to one straight line or more than one, and therefore many more equations with many more points can be generated (with the points found at the intersections of straight lines being optimal).

3. Results

The algorithm developed uses only the coordinates of points and IOPs are therefore not required, which means that it is possible to correct images of unknown origin (scanned form a textbook, video frames, etc.). In this section we will therefore analyze two different cases. For the first case a photograph has been taken using a handheld, non-metric camera (photographing a common scene), which will be used to check the method's accuracy depending upon the number of coefficients calculated. For the second case, photos were taken of a calibration grid using a semi-metric camera designed for engineering purposes, with this portion of the study used to check the method's accuracy versus the most widely used software applied in this type of work. Because no internal parameters are used, no data are shown for either of the cameras.

3.1. Applying the algorithm to a photo from a handheld (non-metric) camera

In order to check the accuracy of the algorithm in relation to the number of coefficients calculated, we have taken a photograph of a normal scene with a handheld camera, with the photo including a favorable type of object (one large rectangular element that occupies almost the entire image). Points were measured on the straight lines of the object, which appear curved in the image. In order to assess the accuracy with which the algorithm corrects the image (depending upon the options proposed), different configurations of points were taken on the same element, progressively increasing the redundancy in the calculation. First 3 points were taken on each edge, then 4 points, and finally 8 points, with different adjustments made in each case (Fig. 2).

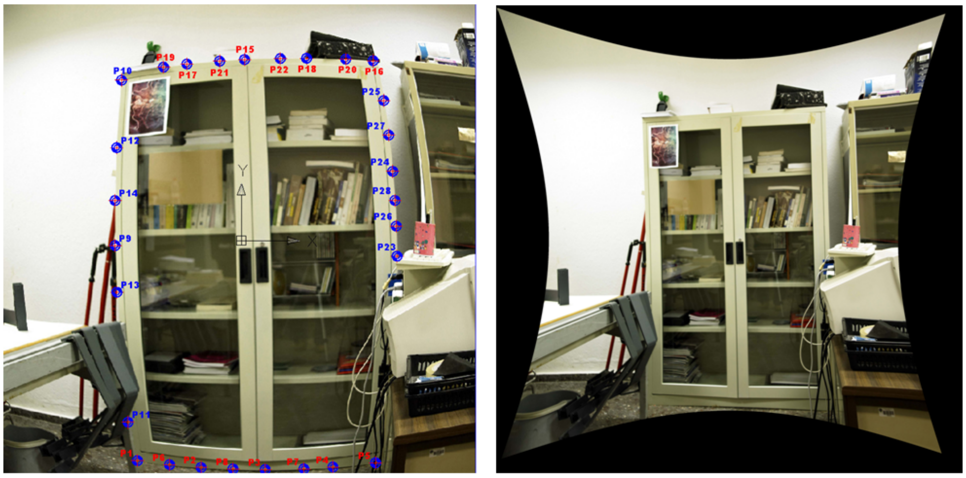

Figure 2. a) Image with distortion and with 28 points measured (on 4 straight lines).
b) Image distortion corrected using the algorithm developed.

The results obtained for the distortion coefficients and PBS decentering value using (8) are shown in Table 1 below for each case.

Distance from the origin	**Distortion (Adjustment using 3 points)**	**Distortion (Adjustment using 4 points)**	**Distortion (Adjustment using 8 points)**
0	0.00	0.00	0.00
100	-3.58	-2.99	-3.06
200	-6.82	-5.73	-5.86
300	-9.37	-7.92	-8.11
400	-10.90	-9.30	-9.52
500	-11.07	-9.55	-9.78
600	-9.54	-8.34	-8.55
700	-5.96	-5.30	-5.43
800	0.00	0.00	0.00
900	8.69	8.01	8.23
1000	20.45	19.27	19.80
Coefficient *a*	-3.63472e-2	-3.03821e-2	-3.10661e-2

Coefficient *b*	5.67924e-8	4.36000e-8	4.44000e-8
Coefficient *c*	---	6.05000e-15	6.47000e-15
Coefficient *P1*	---	---	8.33e-10
Coefficient *P2*	---	---	-6.42e-10
dx_{PBS}	---	---	44.5
dy_{PBS}	---	---	30.2

Table 1. Distortion coefficients and PBS decentering values resulting from the adjustment with lines defined by 3 points, 4 points and 8 points (expressed as pixels).

The results for the radial distortion coefficients show significant variation in the *b* coefficient between the 3-point adjustment and the other two. On the other hand, the variations in coefficient *b* and coefficient *c* between the 4-point adjustments and the >4 point adjustments are minimal. Calculation of the tangential distortion and decentering of the PBS is only possible in the case with >4 points (see section 2.2.4). Therefore, the adjustment of straight lines using 3 points is possible, but the accuracy is insufficient and it does not allow calculation of the *c* coefficient, the value of which is shown to be relevant in the distortion curve, whereas when using 4 points or more this is possible (Fig. 3).

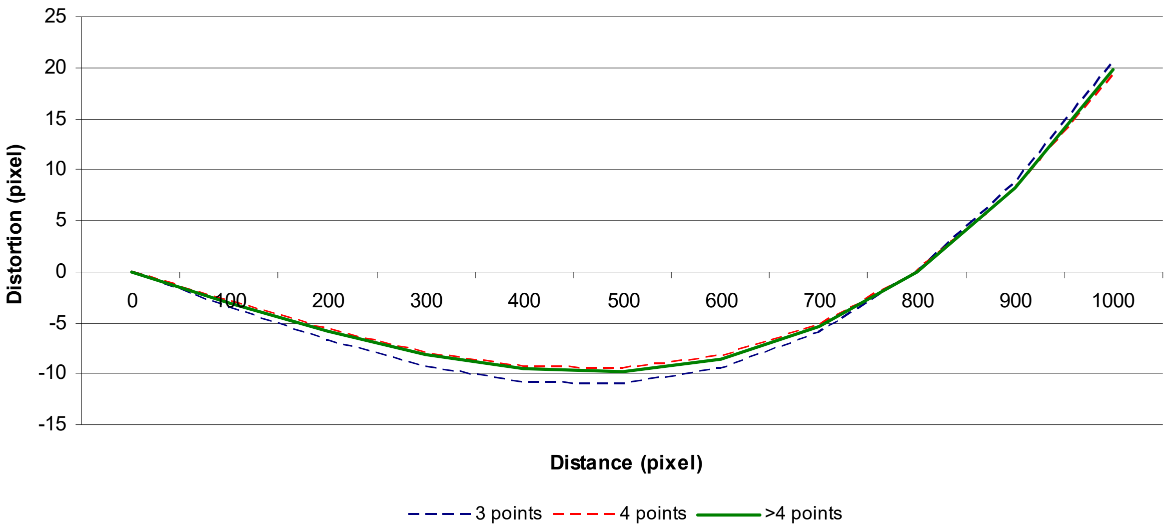

Figure 3. Distortion curves obtained by adjustment using straight lines with 3 points (blue), 4 points (red) and >4 points (green).

In these processes it is necessary to stablish null distortion, having three possibilities: it is possible to stablish null distortion at the beginning (distance = 0), it is possible to stablish just the half area of the photogram inside dr=0 and the other half outside dr=0, or it is possible to stablish null distortion at any point. As it can be seen in Figure 3, in this case the second option has been chosen.

Since the coordinate measurements can be taken very quickly using any image processing software, it is logical to always perform redundant measurements so that the best possible settings can be obtained and the accuracy can be analyzed using reliability tests. Using the 4 straight lines measured in the image in this case, if all of the points are used the resulting system has 20 equations (the first and third lines have 8 points and each generate 6 equations, the second and fourth lines have 6 points and each generate 4 equations), and there are 2 unknowns for distortion (*b* and *c*), 2 for PBS decentering (*dx* and *dy*), and 2 for tangential distortion (*P1* and *P2*). This means that as seen in Table 2 there are 14 redundancies obtained for the equations.

	Eq. 1	**Eq. 2**	**Eq. 3**	**Eq. 4**	**Eq. 5**	**Eq. 6**
Line 1 (points 1-8)	0.62	0.51	0.75	0.79	0.62	0.51
Line 2 (points 9-14)	0.76	0.70	0.75	0.79	---	---
Line 3 (points 15-22)	0.69	0.82	0.59	0.68	0.76	0.59
Line 4 (points 23-28)	0.74	0.80	0.74	0.78	---	---

Table 2. Particularized redundancies obtained for each equation in each line measured

The plot of the cofactor matrix of the residuals characterizes the contribution of each coordinate to the system, resulting in the cofactor matrix diagonal of the residuals (Table 3).

	Line 1		**Line 2**		**Line 3**		**Line 4**	
	x	**y**	**x**	**y**	**x**	**y**	**x**	**y**
1st point	0.00	0.14	0.62	0.00	0.12	0.54	0.39	0.00
2nd point	0.12	0.49	0.27	0.00	0.00	0.19	0.62	0.00
3rd point	0.11	0.47	0.39	0.00	0.08	0.46	0.28	0.00
4th point	0.12	0.45	0.52	0.00	0.13	0.46	0.57	0.00
5th point	0.00	0.13	0.53	0.00	0.00	0.35	0.54	0.00
6th point	0.11	0.47	0.66	0.00	0.12	0.45	0.64	0.00
7th point	0.12	0.48	---	---	0.11	0.54	---	---
8th point	0.11	0.46	---	---	0.13	0.49	---	---

Table 3. The cofactor matrix diagonal of the residuals for each measured point in each line (expressed as pixels)

Based upon their smaller values it can be seen that lines 2 and 4 are nearly vertical and it is the x-coordinate that affects the issue. Similarly, lines 1 and 3 are nearly horizontal and it is the y-coordinate that really causes the problem. The residuals obtained and their values according to the Baarda test result are shown for the first line in Table 4.

Line 1	**Coordinate**	**Residual**	**Baarda Test value**
1st point	X	0.01	2.50
	Y	0.21	2.92

2nd point	X	-0.01	0.17
	Y	-0.37	1.52
3rd point	X	-0.03	0.54
	Y	0.36	1.53
4th point	X	0.02	0.33
	Y	-0.39	1.74
5th point	X	0.01	2.50
	Y	0.14	2.19
6th point	X	0.01	0.18
	Y	0.16	0.68
7th point	X	-0.03	0.50
	Y	-0.18	0.75
8th point	X	0.04	0.71
	Y	0.12	0.52

Table 4. Residuals obtained (expressed as pixels) and associated Baarda Test values for each coordinate of each point on Line 1.

Analysis of the lines 2, 3, and 4 can be performed in the same way. This method thus enables us to study the redundancy of any point, whether it belongs to *n* straight lines or not. We can also obtain the redundancy of each equation for each of the lines regardless of which points may affect it. If any equation or point has a small redundancy, we can study the geometry that causes this and add more points or improve the positions of the measured points.

Once the calculations are complete the covariance matrix can be obtained for the unknowns, which can then be used to calculate the accuracy of each of the corrected coordinates or vector positions in the image. Table 5 shows the application of 4 values for *r*.

r	σ_r
0	0.40
500	0.44
1000	1.65
1500	6.61

Table 5. Standard deviation values for the position of a distortion-corrected point (expressed as pixels).

3.2. Applying the algorithm when using a calibration grid for engineering purposes (semi-metric camera)

Now that the algorithm and its capability for analysis have been validated, its accuracy can also be confirmed using a calibration process (for both the typical and most demanding circumstances in which it will be applied) by means of a grid. Camera calibration is a basic task in photogrammetry that is usually carried out by using calibration grids, and in this case we make use the Photomodeler® calibration grid). This grid will provide high data density in order to generate very precise redundant calculation systems (Fig. 4). We then compare the results obtained using the algorithm presented in this paper to the results obtained using Photomodeler® as well as those obtained by using other algorithms based on plumb-line methods.

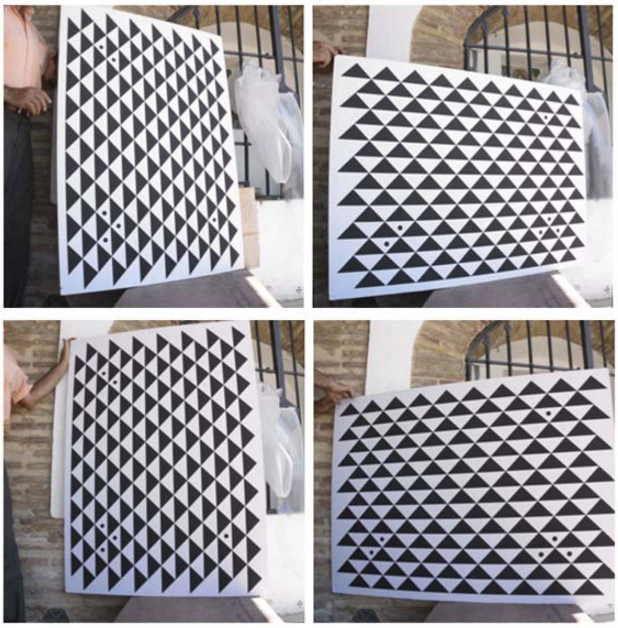

Figure 4. A sample of the images using the Photomodeler® calibration grid (out of ten total).

This comparison was initiated by taking a total of ten photographs of a calibration grid with 121 marks. Next we calculated the distortion coefficients and PBS decentering value using the newly developed algorithm as well as by using Photomodoler® software (which is conventionally used in this type of work) in order to analyze the results.

In both cases the calculation was performed using the total number of points, and in both cases we also used the Photomodeler® automatic measurement points in order to make use of the same observables, so that any variations obtained could only be caused by the algorithms. The total number of lines employed in each of the images was of 56 (30 horizontal or vertical lines and 26 diagonal lines). Table 6 presents a comparison of the results obtained using the newly developed algorithm and those obtained using Photomodeler®.

	dx_{PBS}	dy_{PBS}	Coefficient *b*	Coefficient *c*	Coefficient *P1*	Coefficient *P2*	σ_0
Adjustment using 1 image (60 lines)	24.11	-12.61	1.813e-4	-7.792e-7	6.479e-6	-13.91e-6	0.236

Adjustment using 3 images (180 lines)	21.32	-15.62	1.794e-4	-7.842e-7	6.406e-6	-14.21e-6	0.324
Adjustment using 6 images (360 lines)	26.49	-24.65	1.789e-4	-7.764e-7	6.314e-6	-12.36e-6	0.339
Adjustment using 10 images (600 lines)	19.44	-20.11	1.787e-4	-7.751e-7	6.308e-6	-13.90e-6	0.352
Photomodeler®	---	---	1.804e-4	-7.737e-7	6.232e-6	-13.13e-6	0.472

Table 6. Coefficients resulting from adjustment using the new algorithm (with 1 image, 3 images, 6 images, and 10 images) and using Photomodeler®.

The differences obtained for the values of the PBS are seen in Table 6. Photomodeler® does not include this calculation; instead it calculates the principal point of autocollimation (PPA) and uses this as an approximation for the PBS. With respect to the differences seen in the coefficients of tangential distortion compared to Photomodeler®, these are also negligible since for radius values of 1000 pixels they are all less than 1 pixel (Table 7).

Tangential distortion at 1000 pixels	***Difference versus Photomodeler®***
15.34	0.81
15.59	0.95
13.88	-0.65
15.32	0.79
14.53	0.00

Table 7. Differences in tangential distortion (expressed as pixels).

The graph below shows the distortion polynomials resulting from the previous calculation (Table 6) and their differences from those calculated using Photomodeler® (Fig. 5):

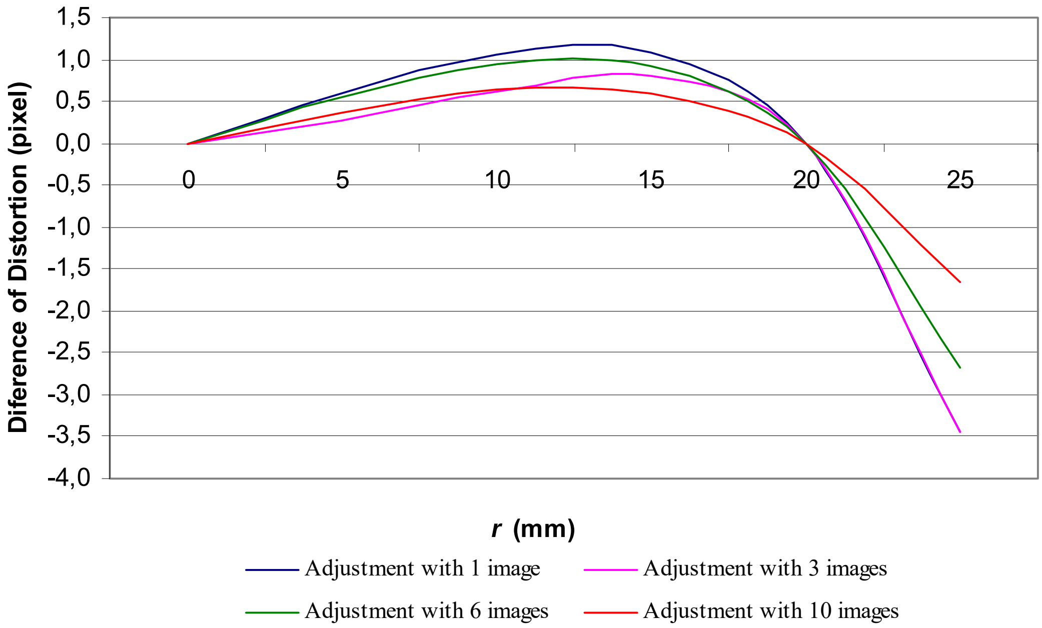

Figure 5: Distortion differences obtained in the four settings using the new algorithm (Table 2) with respect to Photomodeler®

As before, null distortion has to be stablished too. In this case we have stablished it at 20mm distance (being approximately a half of the photogram area). In Table 6 it can be seen that when compared to the adjustment using 10 images, the adjustment made using a single image presents a maximum deviation of 1.4% for coefficient *b* and 0.53% for coefficient *c*, while with Photomodeler® the absolute variations in the solution offered under the different settings show maximum differences of 0.9% for coefficient *b* and 1.3% for coefficient *c*. Based upon these results (taking into account that the same observables were used), and noting that the change in the accuracy of the adjustment can be considered to be no more than 1.5% when using more than one image, we can say that the algorithm successfully solves the determination of distortion using a single image, while Photomodeler® requires a minimum of 6 to provide a reliability similar to that obtained according to our statistical indicators (standard deviations of 0.236, 0.324, and 0.352 for the adjustments using 1, 3, and 10 images, respectively). Figure 6 shows the resulting images of the calibration grid after correcting distortion using the new algorithm developed.

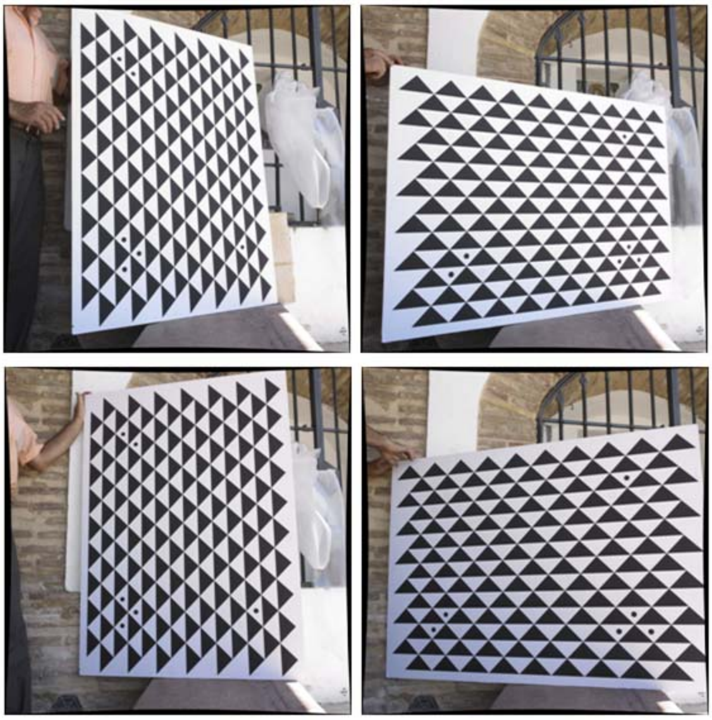

Figure 6. Corrected images of the calibrated grid (out of ten total).

With respect to the traditional algorithms based on plumb-lines, a sample of the previous calculation can be seen below. Four lines have been used, where points 1, 2, 3, and 4 each belong to two straight lines (Fig. 7). With traditional methods these would have to be eliminated since their residuals would differ depending upon which line they were considered as belonging to, while with the new algorithm developed as (8), the same residual value is obtained regardless of the line considered (Table 8).

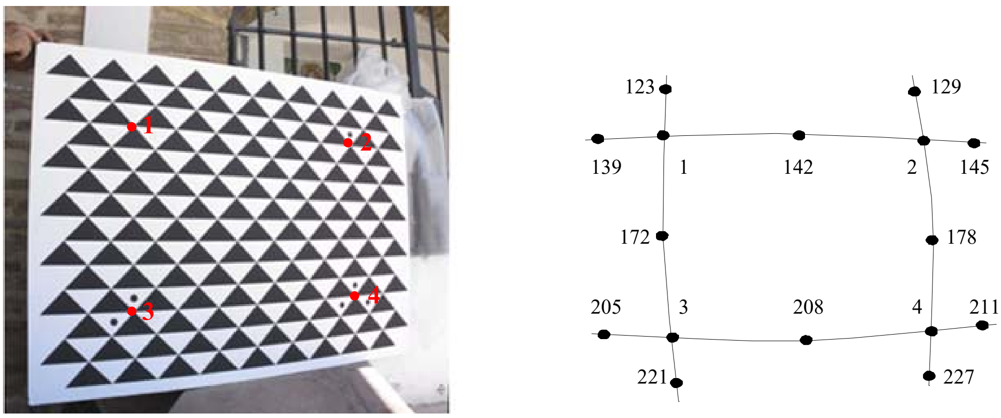

a) b)

Figure 7. a) Calibration grid with 16 points selected for calculation of distortion. Points 1, 2, 3, and 4 each belong to two straight lines. b) Scheme defined for points and straight lines.

		New algorithm, (8)		Traditional algorithms	
Line	**Point**	**Residual x**	**Residual y**	**Residual x**	**Residual y**
Line 1	1	0.22	0.23	0.00	-0.22
	2	-0.17	-0.17	-0.00	-0.16
	139	0.00	-0.41	0.00	0.39
	142	0.00	0.36	0.00	0.36
	145	-0.01	-0.32	-0.01	-0.32
Line 2	3	-0.12	0.16	-0.01	0.16
	4	0.26	-0.14	0.00	-0.15
	205	0.03	-0.40	0.01	-0.40
	208	-0.00	0.32	-0.00	0.32
	211	-0.01	0.11	-0.01	0.10
Line 3	1	0.22	0.23	0.23	0.00
	3	-0.12	0.16	-0.12	0.00
	123	-0.23	0.00	-0.23	0.00
	172	-0.18	-0.00	-0.18	-0.00
	221	0.25	0.01	0.25	0.01
Line 4	2	-0.17	-0.17	-0.17	-0.00
	4	0.26	-0.14	0.25	-0.00
	129	0.11	0.00	0.10	0.00
	178	-0.16	0.01	-0.16	0.01
	227	-0.04	-0.01	-0.04	-0.01

Table 8. Residuals calculated using the two methods, for points that define the four lines in the image that contain common points (expressed in pixels).

4. Conclusions

The algorithm proposed has been shown to be valid and the process of application has proven to be simple and quick, since it only requires measurement of a series of points aligned along different lines in the image (which are straight lines in the object space). The method can be applied manually in the case of conventional scenarios or else automatically when using calibration grids.

The adjustment process requires the start and end of each line to be defined so that our software can calculate the possible combinations of lines with intermediate points (horizontal, vertical, and diagonal). In cases where a calibration grid is employed, the availability of points always allows calculation by least squares. However, if only a common scene is available the lines can be measured manually, with a variable number of points defined depending on the length of each line. In any event, use of the new algorithm is perfectly feasible in either case. However, it is clear that the most reliable distortion calculation will involve the use of a calibration grid, since the redundancy of data is huge and the distribution of points is optimal.

The results obtained show that accuracy is very high even when using only a single image (in the case where multiple straight lines with more than four points are used), while with Photomodeler® a series of images taken from different positions is required. Our algorithm presents this advantage because the number of equations it generates is much higher (there are many more possible combinations of straight lines than collinearity equations), which produces a more precise adjustment in cases where the number of observables is limited. It also allows the PBS to be calculated in a single joint calculation process. Given that the PPA is a point that is found as a projection of the optical center onto the Reseau plate, its position neither depends upon nor affects the geometric characteristics of the image (it cannot be obtained for reasons related to distortion of straight lines). Instead the PBS, which does contain the characteristics of symmetry from the distortion in the image, can be obtained by image analysis. Since the precision obtained from calculation of the PBS does not tend to be high, the majority of the programs used approximate it as being equal to the PPA. In metric cameras it is obviously not possible to calculate the PBS since there is no radial distortion (and therefore it is impossible to determine the point from which there is greatest symmetry in something that does not exist). Furthermore, although our process is less automated compared to the use of Photomodeler® (when using a calibration grid), it can be applied in all cases, both in common scenes and when using calibration grids, as well as with a single image and/or with a small amount of points.

Unlike other methods based upon plumb-lines, our method does not depend on the direction of the lines in the image, because it only uses point coordinates for its calculations, and these are independent of the direction or position of the lines within the scene. Additionally, it is possible to use points that belong to multiple straight lines at the same time, since the calculation of residuals is unique for each point. This means that there are no inconsistent equations in the calculation system that will assign different residuals to the same point when it lies on different straight lines.

References

[1] O. Faugeras, Three-dimensional Computer Vision: A Geometric Viewpoint, MIT Press, Cambridge, Massachusetts, 1993.

[2] JG. Fryer, Close Range Photogrammetry and Machine Vision, K.B.Atkinson, Whittles, Caithness, 1996.

[3] K. Krauss, J. Jansa and H. Kager, Photogrammetry. Volume 2. Advanced Methods and Applications, Dümmler, Bohn, 1997.

[4] PR. Wolf and BA. Dewitt, Elements of Photogrammetry with Applications in GIS, Thrid edition, McGraw-Hill, New York, 2000.

[5] R. Hartley and A. Zisserman, Multiple View Geometry in Computer Vision, Cambridge University Press, Cambridge, 2003.

[6] TA. Clarke and JG. Fryer, “The development of camera calibration methods and models,” Photogrammetric Record 16(91) (1998) 51-66.

[7] F. Remondino and C. Fraser, “Digital camera calibration methods: considerations and comparisons,” International Archives of Photogrammetry, Remote Sensing and Spatial Information Sciences 36(5) (2006) 266-272.

[8] DC. Brown, “Close-range camera calibration,” Photogrammetric Engineering and Remote Sensing 37(8) (1971) 855-866.

[9] YI. Abdel-Aziz and HM. Karara, Direct linear transformation from comparator coordinates into object-space coordinates in close-range photogrammetry, American Society of Photogrammetry Symposium on Close-Range Photogrammetry, Urbana, Illinois, 1-18.

[10] Z. Zhang, A flexible new technique for camera calibration, IEEE transactions on Pattern Analysis and Machine Intelligence 22(11) (2000) 1330-1334.

[11] RY. Tsai, A versatile camera calibration technique for high accuracy 3D machine vision metrology using off-the-self TV cameras and lenses, IEEE International Journal Robotics and Automation 3(4) (1987) 323-344.

[12] J. Weng, P. Cohen, and M. Herniou, Camera calibration with distortion models and accuracy evaluation, IEEE Transactions on on Pattern Analysis and Machine Intelligence 16(5) (1992) 469-479.

[13] CS. Fraser, Digital camera self-calibration, ISPRS Journal of Photogrammetry and Remote Sensing 52(4) (1997) 149-159.

[14] DD. Lichti and MA. Chapman, Constrainted FEM self calibration, Photogrammetric Engineering and Remote Sensing 63(9) (1997) 1111-1119.

[15] JG. Frayer and DC. Brown, Lens distortion for close-range photogrammetry, Photogrammetric Engineering and Remote Sensing 52(1) (1986) 51-58.

[16] R. Swaminathan and S. Nayar, Nonmetric calibration of wide-angle lenses and polycameras, IEEE Trans. Pattern Anal. Mach. Intell 22(10) (2000) 1172-1178.

[17] JG. Habib, M. Morgan and YR. Lee, Bundle adjustment with self-calibration using straight lines, Photogrammetric Record 17(100) (2002) 635-650.

[18] E. Rosten and R. Loveland, Camera distortion self-calibration using the plumb-line constraint and minimal Hough entropy, Machine Vision and Applications 22 (2011) 77-85.

[19] J. Herraez, JL. Denia, P. Navarro, J. Rodriguez. and MT. Martin, Epipolar image rectification through geometric algorithms with unknown parameters, Journal of Electronic Imaging 22(4) (2013) 043021.

Figure Captions

Figure 1. Point 1: point corrected for distortion using a residual for measurement error. Points 2 and 3: corrected positions for point 1 by the conventional method based upon the straight line studied. Point 4: position of point 1 corrected using the new algorithm, Eq. (8).

Figure 2. a) Image with distortion and with 28 points measured (on 4 straight lines). b) Image distortion corrected using the algorithm developed.

Figure 3. Distortion curves obtained by adjustment using straight lines with 3 points (blue), 4 points (red) and >4 points (green).

Figure 4. A sample of the images using the Photomodeler® calibration grid (out of ten total).

Figure 5: Distortion differences obtained in the four settings using the new algorithm (Table 2) with respect to Photomodeler®

Figure 6. Corrected images of the calibrated grid (out of ten total).

Figure 7. a) Calibration grid with 16 points selected for calculation of distortion. Points 1, 2, 3, and 4 each belong to two straight lines. b) Scheme defined for points and straight lines.

Table Captions

Table 1. Distortion coefficients and PBS decentering values resulting from the adjustment with lines defined by 3 points, 4 points and 8 points (expressed as pixels).

Table 2. Particularized redundancies obtained for each equation in each line measured

Table 3. The cofactor matrix diagonal of the residuals for each measured point in each line (expressed as pixels)

Table 4. Residuals obtained (expressed as pixels) and associated Baarda Test values for each coordinate of each point on Line 1.

Table 5. Standard deviation values for the position of a distortion-corrected point (expressed as pixels).

Table 6. Coefficients resulting from adjustment using the new algorithm (with 1 image, 3 images, 6 images, and 10 images) and using Photomodeler®.

Table 7. Differences in tangential distortion (expressed as pixels).

Table 8. Residuals calculated using the two methods, for points that define the four lines in the image that contain common points (expressed in pixels).